Spectrochimica Acta Part A: Molecular and Biomolecular Spectroscopy 211 (2019) 239–245

Contents lists available at ScienceDirect

Spectrochimica Acta Part A: Molecular and Biomolecular Spectroscopy

journal homepage: www.elsevier.com/locate/saa

Two coumarin-based turn-on fluorescent probes based on for hypochlorous acid detection and imaging in living cells

Qingming Wang [a,*], Lei Jin [a,b], Wenling Wang [a], Lihui Dai [a], Xiaoxue Tan [a], Cong Zhao [a]

[a] School of Pharmacy, Jiangsu Provincial Key Laboratory of Coastal Wetland Bioresources and Environmental Protection, Yancheng Teachers' University, Yancheng, Jiangsu 224051, People's Republic of China

[b] College of Biotechnology and Pharmaceutical Engineering, Nanjing University of Technology, Nanjing, 210009, People's Republic of China

ARTICLE INFO

Article history:
Received 25 September 2018
Received in revised form 19 November 2018
Accepted 9 December 2018
Available online 10 December 2018

Keywords:
Coumarin-based fluorescence probe
Hypochlorous acid
Reactive species
Mechanism
Cell imaging

ABSTRACT

This work, two turn-on fluorescent probes (3-acetyl-2H-chromen-2-one (**ACO**) & (1E)-1-(1-(2-oxo-2H-chromen-3-yl)ethylidene)thiosemicarbazide (**CETC**)) based on coumarin have been designed and synthesized, which could selectively and sensitively recognize ClO^- with fast response time. **ACO** & **CETC** were almost non fluorescent possibly due to both the lacton form of coumarin and unbridged C═N bonds which can undergo a nonradiative decay process in the excited state. Upon the addition of ClO^-, **ACO** & **CETC** were oxidized to ring - opened by cleavage the C—O and C═N and the fluorescence intensity were increased considerably. Fluorescence titration experiments showed that the detection limit **ACO** & **CETC** is as low as 22 nm and 51 nm respectively. In particular, some relevant reactive species, including •OH, $^1O_2$, H_2O_2, KO_2, some anions and cations cannot be interference with the test. In live cell experiments, **ACO** & **CETC** were successfully applied to image exogenous ClO^- in HepG2 cells. Therefore, **ACO** & **CETC** not only could image ClO^- in living cells but also proved that C—O and C═N can be cleavage by ClO^-.

1. Introduction

Reactive oxygen species (ROS), such as •OH, $^1O_2$, H_2O_2, O_2^-, ClO^- and so on, play important roles in cell signaling and maintaining redox homeostasis [1–5]. Among of the broad range of biologically reactive species mentioned above [6], hypochlorite acid (HClO) is a weakly acidic (pK_a = 7.53) and partially exists in the form of hypochlorite ion (ClO^-) in physiological conditions [7–9]. It is produced by the peroxidation reaction between hydrogen peroxide and chloride ions which was catalyzed by myeloperoxidase (MPO) [10–13]. In view of the highly oxidant property in immune systems, the normal pathology concentration of HClO is <200 μM [14]. The abnormal production of hypochlorite can lead to tissue damage and various of human diseases, including arthritis, hepatic ischemia-reperfusion damage, cardiovascular diseases, rheumatoid, lung injury, cancer, atherosclerosis [15–23]. Due to the importance of HClO, more and more scientists have attracted a great deal of interest to develop new suitable chemical methods for real-time monitoring of HClO or rapid imaging in living systems [24–26].

Due to higher selectivity, better sensitivity, readily operation and potentially of real time monitoring, there are many fluorescence probes developed for the detection of ClO^- [7,27–37]. Unfortunately, most of the reported fluorescence probes can only be operated in the mixture of water and organic solvents, this may be a limiting factor for applications of these probes. So it is still significative to extend a new fluorescent probe for the recognition moiety of ClO^-.

Herein, we reported two coumarin-based probes for ClO^-. The synthesized coumarin derivative **ACO** & **CETC** were followed early reported method with some modify. The **ACO** & **CETC** shown almost non-fluorescent emission which is due to the donor-excited photo induced electron transfer(D-PET)process [38]. However, **ACO** & **CETC** could convert to (Z)-2-(2-hydroxybenzylidene)-3-oxobutanoic acid (**HOA**) in presence of ClO^- (Scheme 1) by breaking the C—O and C═N.

2. Experimental Section

2.1. Materials and Instruments

We purchase all of the reagents from commercial providers and use them without further purification. The anions like Cl^-, Br^-, I^-, SO_4^{2-}, PO_4^{3-}, and so on, came from their sodium salts or potassium salts. The cations, for example, Na^+, K^+, Mg^{2+}, Ca^{2+}, Ba^{2+}, Cr^{3+}, Co^{2+}, and so on, came from their chloride or nitrate, both anions and cations were purchased from Shanghai Experiment Reagent Co., Ltd. (Shanghai, China). The probes 3-acetyl-2H-chromen-2-one (**ACO**) & (1E)-1-(1-(2-oxo-2H-chromen-3-yl)ethylidene)thiosemicarbazide (**CETC**) were prepared according to the literature method with some modify [39–41].

* Corresponding author.
E-mail address: wangqm@yctu.edu.cn (Q. Wang).

https://doi.org/10.1016/j.saa.2018.12.019
1386-1425/

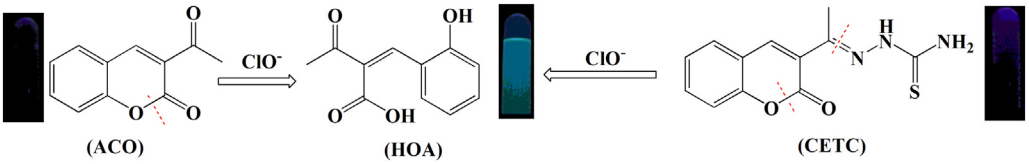

Scheme 1. Mechanism of ClO^- sensing by probe **ACO** & **CETC**.

^1H NMR and ^{13}C NMR spectra were recorded on a Bruker DRX 400 spectrometer with TMS as the internal standard. FT-IR spectrum (4000–400 cm^{-1}) were obtained on NICOLET380 FT-IR spectrometer in KBr disks. Elemental analyses (EAs) were carried out with a VARI-EL elemental analyzer. Electrospray ionization mass spectra (ESI - MS) were measured on a Triple TOF TM 5600^+ system. Fluorescence spectral data were calculated by a RF-5301 fluorescence spectrophotometer. Ultraviolet spectrum was performed on UV-1800 ENG 240 V. Fluorescence images of HepG2 cells were performed using a confocal laser scanning microscope with model LSM-880.

2.2. Absorption and Fluorescence Spectroscopy

ACO & **CETC** were dissolved in DMSO for a stock solution (0.01 M). 5% of H_2O_2 was by dilution of 30% solution in water. KO_2 was diluted in anhydrous DMSO to give $\cdot O_2^-$. $^1O_2$ was obtained by mixing H_2O_2 and 100-exceed of NaClO. $\cdot OH$ was produced by Fenton reaction, mixing H_2O_2 and 10-exceed $(NH_4)_2Fe(SO_4)_2$ [42,43]. Absorption and fluorescence spectrum were recorded in a quartz optical of 1.0 cm optical path length at room temperature. All of the test solutions were prepared by displacing 2 μL of the stock solution into a 2 mL of 20 mM Tris - HCl at $pH = 7.2$.

2.3. Cell Culture and Cell Imaging

HepG2 cells were cultured in Dulbecco's Modified EagleMedium (DMEM) medium supplemented with 10% fetal bovine serum (FBS) and 0.1% antibiotic-antimycoticmix antibiotic and grown at 37 °C in a 5% CO_2. Cells were treated with **ACO** & **CETC** (10 μM) in PBS buffer (2% DMSO, $pH = 7.2$) for 30 min. After, the cells were then incubated with ClO^- (40 μM) for another 40 min. Then the cells were washed with PBS buffer for three times. And the living cell images were captured through a confocal laser scanning microscope. The survivance of HepG2 cells incubated with **ACO** & **CETC** respectively, was determined by the 3-[4,5-Dimethylthiazo-2 -yl]-2,5-diphenpyltetra-zolium bromide (MTT) assay.

2.4. Synthesis of Probe *ACO & CETC*

2.4.1. Synthesis of 3-acetyl-2H-chromen-2-one (*ACO*)

Following the reported method [44,45] to synthesize probe ***ACO***, as showed in Scheme S1. 0.6106 g (5 mmol) 2-hydroxybenzaldehyde and 0.646 g (5 mmol) ethyl 3-oxobutanoate were added to 30.00 mL ethanol. Then piperidine was added drop-wise into the mentioned solution above. After the resulting solution was reflexed for 16 h with a constant stirring, the color of the reaction was dark green and cooled to room temperature, yellow solid was obtained and the precipitation was collected and washed with ethanol for three times and dried *in vacuo*. Yield, 57.2%. FT-IR (KBr, cm^{-1}): 3030 (Ar—H), 2927 (C—H), 1740 (C—O), 1614, 1558, 1454 (Ar, C═C), 1211, 1122 (C—O—C). Exact mass for **ACO**: 188.0473, ESI - MS (positive mode) [**ACO** + H^+] + (m/z,189.0638), [**ACO** + Na^+] + (m/z,211.0486). Elemental analysis (calcd. %) for $C_{11}H_8O_3 \cdot 0.2H_2O$: C, 68.89; H, 4.41; Found: C, 68.76; H, 4.68. ^1H NMR (400 MHz, DMSO) δ 11.22 (s, 1H), 8.67 (s, 1H), 7.96 (dd, $J = 7.7$, 1.4 Hz, 1H), 7.78–7.73 (m, 1H), 7.49–7.40 (m, 2H), 3.34 (s, 1H). ^{13}C NMR (101 MHz, DMSO) δ 195.59 (s), 158.92 (s), 155.08 (s), 147.53 (s), 134.96 (s), 131.26 (s), 125.42 (s), 124.90 (s), 118.65 (s), 116.59 (s), 40.61 (s), 40.40 (s), 40.19 (s), 39.98 (s), 39.78 (s), 39.57 (s), 39.36 (s), 30.54 (s).

2.4.2. Synthesis of (1E)-1-(1-(2-oxo-2H-chromen-3-yl)ethylidene) thiosemicarbazide (*CETC*)

CETC was prepared by mixing of 3-acetyl-2H-chromen-2-one with thiosemicarbazide in a 1:1 ratio in 30 mL ethanol solution. Then a few drops of acetic acid were added drop-wise into the mentioned solution above. The solution was reflux for 12 h. The dark brown color product was filtered off and recrystallized from ethanol solution. The compound was dried in vacuum desiccator. Yield, 36.4%. FT-IR (KBr, cm^{-1}): 3389 (N—H), 3030(Ar—H), 2927 (C—H), 1719 (C═O), 1605, 1497, 1454 (Ar, C═C), 1240, 1116 (C—O—C).Exact mass for **CETC**: 261.0572, ESI - MS (positive mode) [**CETC** + H^+] + (m/z, 262.0804), [**CETC** + H^+] + (m/z, 284.0624). Elemental analysis (calcd. %) for $C_{12}H_{11}N_3O_2S$: C, 55.16; H, 4.24; N, 16.08; Found: C, 55.20; H, 5.18, N, 4.24. ^1H NMR (400 MHz, DMSO) δ 10.63 (s, 1H), 10.46 (s, 2H), 8.48 (s, 2H), 8.43 (s, 2H), 8.02 (s, 1H), 7.97 (s, 2H), 7.77 (d, $J = 8.9$ Hz, 2H), 7.68–7.62 (m, 2H), 7.45–7.37 (m, 4H), 3.44 (dd, $J = 14.0$, 7.0 Hz, 1H), 2.26 (s, 5H), 2.18 (s, 1H), 1.07 (s, 1H), 1.06 (s, 1H), 1.04 (s, 1H). ^{13}C NMR (101 MHz, DMSO) δ 179.70 (s), 159.61 (s), 153.84 (s), 146.43 (s), 142.47 (s), 132.86 (s), 129.59 (s), 126.27 (s), 125.24 (s), 119.42 (s), 116.45 (s), 40.61 (s), 40.40 (s), 40.19 (s), 39.98 (s), 39.77 (s), 39.59 (s), 39.46 (d, $J = 21.0$ Hz), 16.53 (s).

3. Results and Discussion

3.1. Synthesis and Characterization

The synthesis of **ACO** began with 2-hydroxybenzaldehyde and ethyl 3-oxobutanoate which were catalyzed by piperidine. The compound **CETC** was synthesized by using the intermediate **ACO** as reaction material undergoing condensation reaction with thiosemicarbazide. Both **ACO** and **CETC** were recrystalled by CH_2CH_3OH/H_2O to give pure products. Detail characterization data and experimental procedure were shown in the Scheme 2. The structures of **ACO** & **CETC** were confirmed

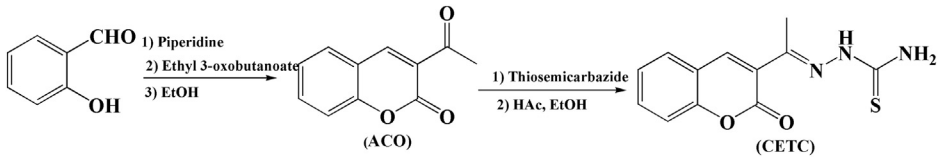

Scheme 2. Design and synthesis of the probe **ACO** & **CETC**.

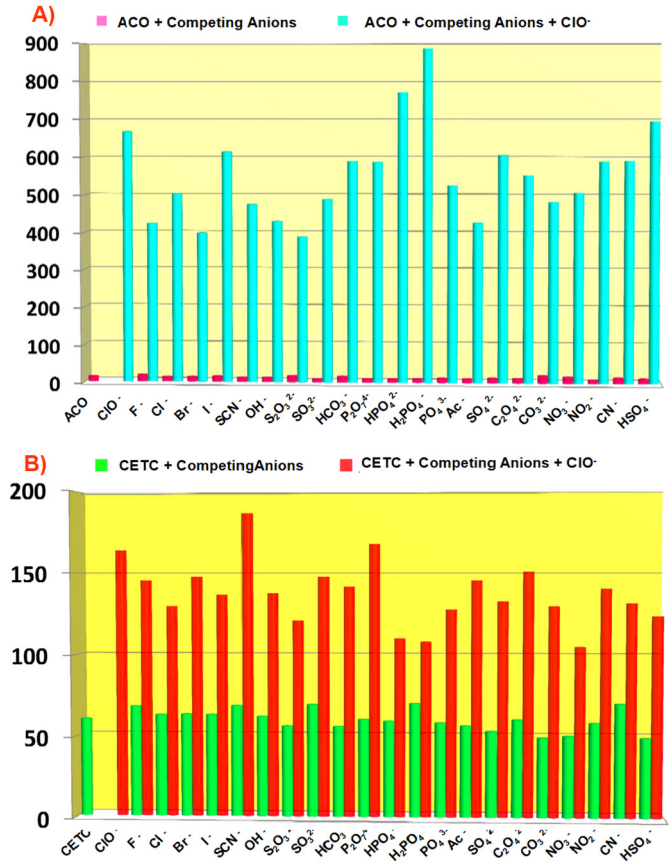

Fig. 1. Examination of selectivity of **ACO** & **CETC** towards ClO^- (1.0 μM) in the presence of various anions (20 equiv.) in Tris - HCl buffer/DMSO (v:v = 9:1, 20 mM, pH = 7.0). A) **ACO**; B) **CETC**.

by Elemental analyses (EAs), FT - IR spectra (IR) analysis, Electrospray ionization mass spectra (ESI - MS), ^{1}H NMR and ^{13}C NMR, (Fig. S1–S8).

3.2. Spectral Characteristics of *ACO* & *CETC* for Various Anions and Cations

To evaluate the anion-binding properties of **ACO** & **CETC**, a wide range of environmentally and physiologically anions and cations were investigated using the fluorescence spectra. The solution of **ACO** & **CETC** (1.0 μM) and added separately 20 equiv. selected anions, such as Cl^-, Br^-, I^-, SO_4^{2-}, PO_4^{3-}, $H_2PO_4^-$, OH^-, HCO_3^-, NO_3^-, $C_2O_4^{2-}$, F^-, HPO_4^{2-}, $S_2O_3^{2-}$, NO_2^-, Ac^-, $P_2O_7^{4-}$, $B_4O_7^{2-}$, CO_3^-, HSO_3^-, SO_3^{2-}, it is evident that the addition of these anions to the solution of **ACO** & **CETC**, there was almost no effect on the fluorescence emission enhancement was found. But when 5.0 equiv. ClO^- was added, the fluorescence emission of **ACO** & **CETC** was increased rapidly. Thus, **ACO** & **CETC** exhibited excellent selectivity for ClO^- over the tested anions. The competitive studies of **ACO** & **CETC** were conducted with the addition of 5.0 equiv. ClO^- to induced fluorescence enhancement before mixed 20 equiv. of Cl^-, Br^-, I^-, SO_4^{2-}, PO_4^{3-}, $H_2PO_4^-$, OH^-, HCO_3^-, NO_3^-, $C_2O_4^{2-}$, F^-, HPO_4^{2-}, $S_2O_3^{2-}$, NO_2^-, Ac^-, $P_2O_7^{4-}$, $B_4O_7^{2-}$, CO_3^-, HSO_3^-, SO_3^{2-}, respectively. The fluorescence emission of the mixed system at 478 nm was showed in Fig. 1, it was demonstrated that the co-existent anions impacted a negligible effect on the recognition of the **ACO** & **CETC** with ClO^-. In the same way, some selected cations, such as Na^+, K^+, Mg^{2+}, Ca^{2+}, Ba^{2+}, Cr^{3+}, Co^{2+}, Mn^{2+}, Fe^{3+}, Ni^{2+}, Cu^{2+}, Cd^{2+}, Zn^{2+}, Al^{3+}, Pb^{2+}, Bi^{3+}, Ag^+, Sn^{2+}, Sr^+, NH_4^+, Hg^{2+}, were also tested. The results revealed that all the tested cations could not interfere the **ACO** & **CETC** to recognize the ClO^-(as showed in Fig. S9–Fig. S14). Thus, the dramatic response suggested that **ACO** & **CETC** were highly selective and selective fluorescence probe for ClO^- in our prospective.

3.3. UV–vis absorption spectra of *ACO* & *CETC* towards ClO^-

The Uv-vis spectras of **ACO** & **CETC** was examined in Tris - HCl buffer/DMSO (v:v = 9:1, 20 mM, pH = 7.0). Uv-vis spectra of **ACO** (10 μM) exhibited nearly no absorption. After the treatment of ClO^- at room temperature, the absorption peak at 407 nm obviously increased gradually, a new absorption peak was present at 407 nm, with the increasing of ClO^-, the absorbance at 407 nm was gradually increased (Fig. 2A). Besides, a color change from colorless to yellow can be visualized clearly by naked eye. Fig. 2B showed the Uv-vis spectra of **CETC** (10 μM), which exhibited an absorption maximum at λ = 334 nm and λ = 257 nm. When the solution of ClO^- was titrated into Tris - HCl buffer/DMSO (v:v = 9:1, 20 mM, pH = 7.0) containing **CETC**, the maximum absorption peak at 354 nm was declined gradually, and another absorption peak at 257 nm was increased gradually.

3.4. Fluorescence Spectra of *ACO* & *CETC* towards ClO^-

The fluorescent emission spectrum was monitored by titration experiment with various concentrations of ClO^-. As showed in Fig. 3A, for free **ACO** (1.0 μM), no obvious emission was observed with the excitation at 420 nm in the detection system. It was interesting to us that with the incremental changes of ClO^- (0–8.0 μM) brought about a significant fluorescence turn-on response at 478 nm with a visual fluorescence change from colorless to blue. There was an approximately 36-fold increasing could be observed. From Fig. 3B we could find that **CETC** (1.0 μM) display very weak fluorescence at 495 nm when it was

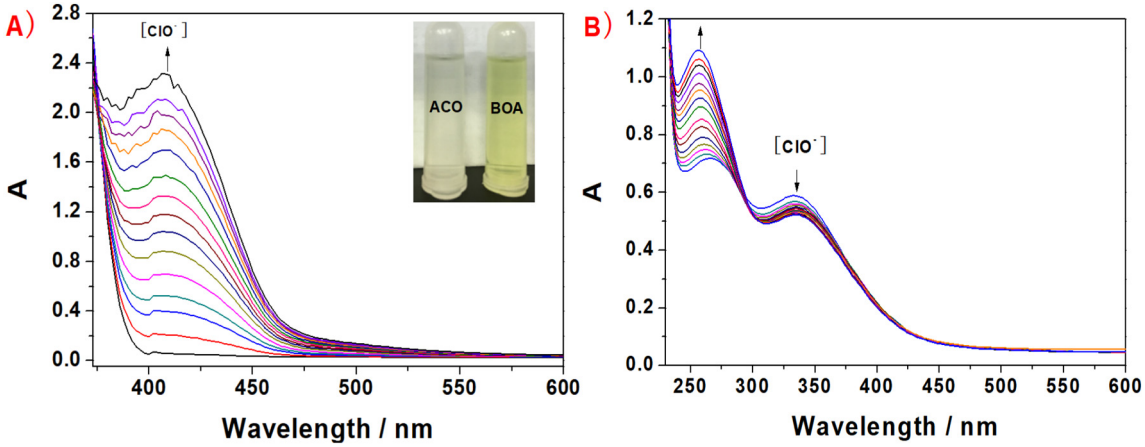

Fig. 2. Changes in the absorption spectra of **ACO** & **CETC** in the presence of ClO^-.

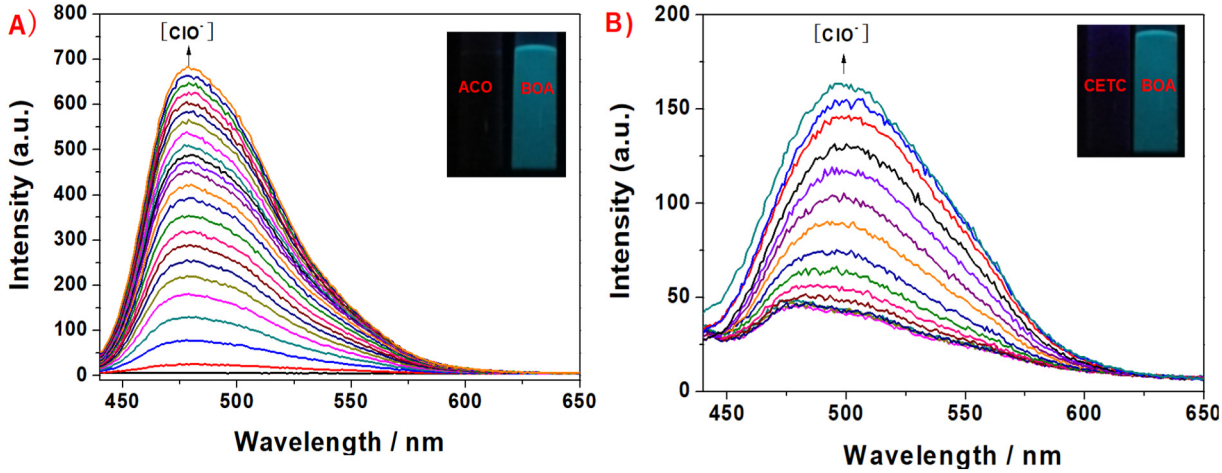

Fig. 3. Fluorescence titration of **ACO** & **CETC** (1.0 μM) with different concentration of ClO^- in Tris - HCl buffer/DMSO (v:v = 9:1, 20 mM, pH = 7.0) solution. Inset: the change of fluorescence depending on the concentrations of ClO^- by illumination with a 365 nm UV lamp.(A) for **ACO**; (B) for **CETC**.

excited at 380 nm, the fluorescence emission was enhanced gradually with the various concentrations of ClO^- was titrated. It is about 3-fold increasing could be found. Compared with **ACO** & **CETC**, we could find that probe **ACO** caused more fluorescence enhancement than **CETC**. The quantum yield was 82.05% and 14.25%, respectively (Fig. S15). The fluorescence variation experiment indicated that **ACO** & **CETC** were enough to detect the concentration of ClO^-.

By the fluorescence titration method, the sensitivity of **ACO** & **CETC** to ClO^- was well examined by using the working curve. As showed in Fig. 4A & B, 1.0 μM of **ACO** & **CETC** were treated with various concentrations of ClO^- (0–8.0 μM) in Tris - HCl buffer/DMSO (v:v = 9:1, 20 mM, pH = 7.0). The correlation coefficient of R^2 is 0.998 and 0.996, respectively. The detection limit (LOD) for ClO^- by **ACO** & **CETC** based on the definition by IUPAC (CDL = 3 Sb/m) were calculated to be 22 nM and 51 nM, respectively. The lower LOD is similar to the early results [43,46,47] and better than other result [48] (as showed in Table S1). The results meant that **ACO** & **CETC** could be potentially applied to detect ClO^- quantitatively. Moreover, there was also demonstrated that **ACO** & **CETC** to be very highly sensitive probe for ClO^-.

Furthermore, the response time of **ACO** to ClO^- was also performed. A plot of fluorescence intensity *vs* time was showed when **ACO** is titrated with 0, 1.0 μM, 2.0 μM of ClO^-, respectively. Within the time of 0–30 s, the fluorescence intensity increased with the time and when the time reached 30 s, the fluorescence intensity was reached to the maximum. The maximum could be maintained for 5 min (Fig. S16).

3.5. Selectivity Studies over some Oxidative Species

Next, parallel experiments for specificity of **ACO** & **CETC** towards ClO^- over other ROS (·OH, $^1O_2$, H_2O_2, KO_2) were carried out. The **ACO** & **CETC** barely showed any fluorescence enhancement in response to hydroxylradical(·OH), singlet oxygen ($^1O_2$), H_2O_2, potassium superoxide (KO_2^-). While the ClO^- was added to the solution of **ACO** & **CETC** in Tris - HCl buffer/DMSO (v:v = 9:1, 20 mM, pH = 7.0), an obviously enhanced fluorescence at 478 nm (for **ACO**, 498 nm for **CETC**) was obtained. The results indicated that the reactive oxygen species ·OH, ClO^-, $^1O_2$, H_2O_2, KO_2 cannot interference the test results. As showed in Fig. 5, the relative enhancement of fluorescence emission caused by ClO^- was 24-fold (for **ACO**, 2-fold for **CETC**), which was much higher than other oxidative species. These results manifested that **ACO** & **CETC** could detect ClO^- not only qualitatively but also quantitatively in complex biological systems.

3.6. Cell Imaging

Inspired by the favorable fluorescence response of **ACO** & **CETC** to ClO^-, fluorescent imaging of ClO^- using **ACO** & **CETC** in living HepG2 were determinated. Initially, the cytotoxicity of **ACO** & **CETC** were recorded by using the MTT assay to evaluate the possibility of probes to be applied to living HepG2 cells. As showed in Fig. S17, both of the survival rates of cell remained >90% after incubating with **ACO** or **CETC** in

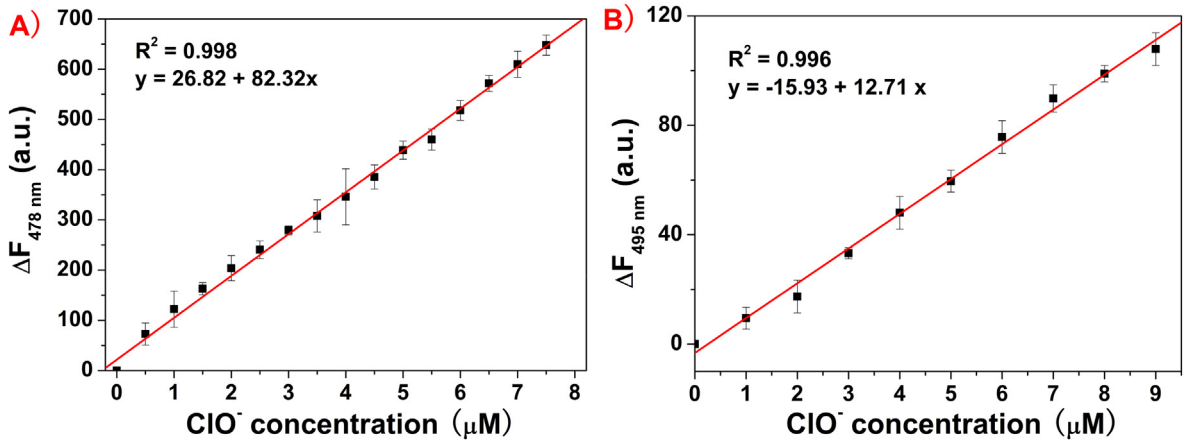

Fig. 4. Fluorescent emissions spectra of **ACO** & **CETC** (1.0 μM) in the presence of ClO^-.(C) for **ACO**; (D) for **CETC**.

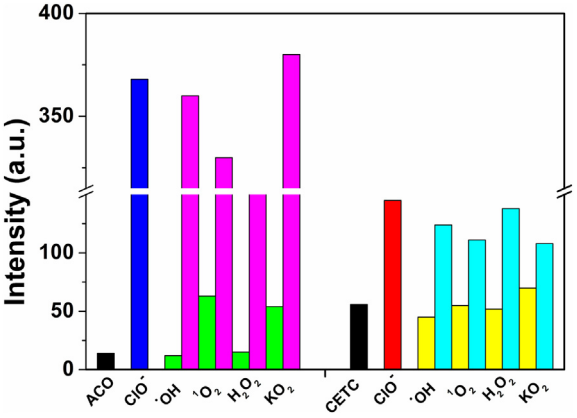

Fig. 5. Fluorescence response of **ACO** & **CETC** (1.0 μM) to NaClO (5 μM) with the competition analytes.

range of 0–60 μM for 24 h, revealing that **ACO** & **CETC** have almost no remarkable cytotoxicity to HepG2 cells, and can be used to biological body. Then the ability of **ACO** or **CETC** to image ClO^- in HepG2 cells was evaluated. From Fig. 6 and Fig. 7, HepG2 cells were incubated with 10 μM of **ACO** or **CETC** for 30 min at 37 °C displayed no obvious fluorescence for **ACO** or weak blue fluorescence for **CETC**. After incubation of the probes treated HepG2 cells with 40 μM ClO^- for another 40 min, strong blue fluorescence image of **ACO** and **CETC** was found through the fluorescent micro-scope. Therefore, **ACO** & **CETC** were cell membrane permeable and have potential applicability for detecting ClO^- in living cells.

3.7. Proposed Mechanism

The mass spectrometry is widely used to analyze the product between **ACO** & **CETC** and ClO^- in CH_3OH/H_2O(v:v = 1: 9). Scheme 1 shows the product **HOA** is formed after the reaction between **ACO** and ClO^-. From Fig. 8 we could find that a peak at m/z = 239.1753, corresponding to [**HOA** + H + CH_3OH]$^+$ (cal. M/z = 239.1519), a peak at m/z = 261.0678, corresponding to [**HOA** + Na + CH_3OH] + (cal. M/z = 261.0739), a peak at m/z = 301.1594, corresponding to [**HOA** + Na + $4H_2O$] + (cal. M/z = 301.1556), and a peak at m/z = 360.3465, corresponding to [**HOA** + $5H_2O$ + $2CH_3OH$] (cal. M/z = 360.3602) are clearly observed, which suggested that the C—O of **ACO** could be cleaved by the oxidation of ClO^-. For the mechanism between **CETC** and ClO^- is also investigated by mass spectrometry in CH_3OH/H_2O(v:v = 1: 9). From Fig. S18, a peak at m/z = 239.1750 corresponds to [**HOA** + H + CH_3OH] + (cal. M/z = 239.1519), a peak at m/z = 301.1594, corresponding to [**HOA** + Na + $4H_2O$] + (cal. M/z = 301.1556), and a peak at m/z = 360.3456, corresponding to [**HOA** + $5H_2O$ + $2CH_3OH$] (cal. M/z = 360.3602) are clearly observed, which indicated that the C—O and C═N of **CETC** could also be cleaved by the oxidation of ClO^-. These results demonstrated that ClO^- could cleave the C—O and C═N by oxidation.

4. Conclusions

In conclusion, we have successfully synthesized two turn-on fluorescent probes (**ACO** & **CETC**) for highly sensitive detection of ClO^- with fast response time by oxidative cleavage of C—O and C═N. The **ACO** & **CETC** displayed high selectivity for ClO^- over other anions and cations with a detection limit of 22 nM and 51 nM, respectively. What is more, some relevant reactive species, including ·OH, $^1O_2$, H_2O_2, KO_2 could not interference the test results. More importantly, these probes can sense intracellular ClO^- levels.

Acknowledgments

This work are financially supported by the National Natural Science Foundation for Young Scientists of China (21301150), the Practice Innovation Training Program Projects for the Jiangsu College Students

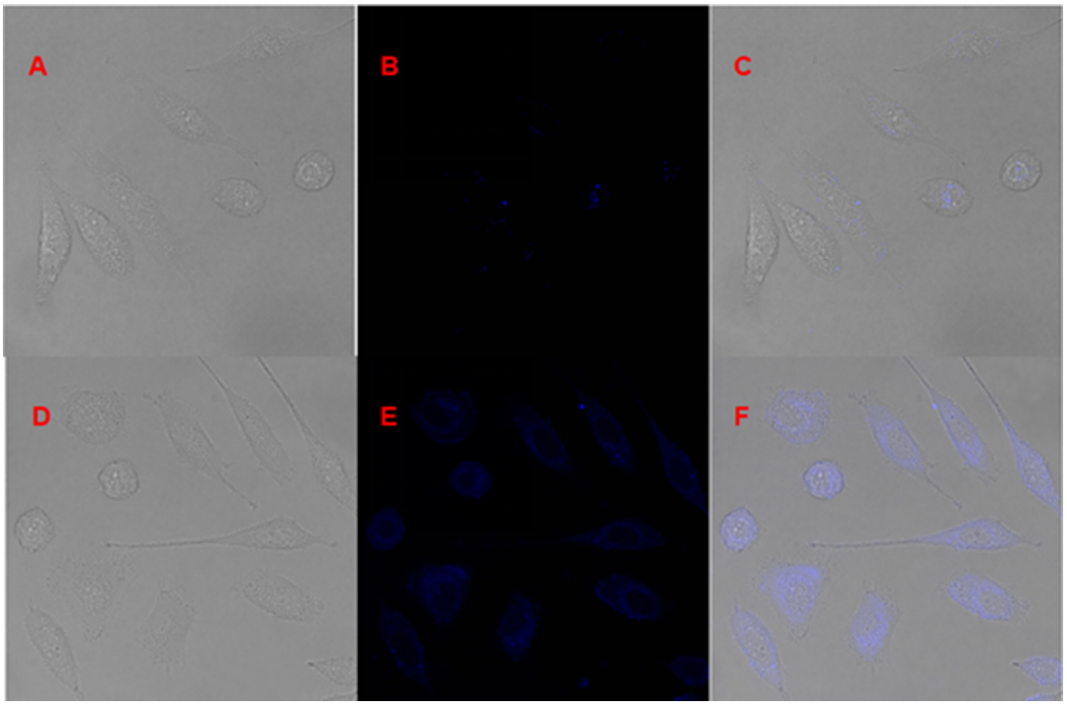

Fig. 6. Fluorescence microscopic images of HepG2 cells: (a) Untreated Cell control; (b) Cells treated with HL; (c) overlap image of (a) and (b); (d) Untreated Cell control; (e) Cells treated with **ACO** and ClO^-; (f) overlap image of (d) and (e).

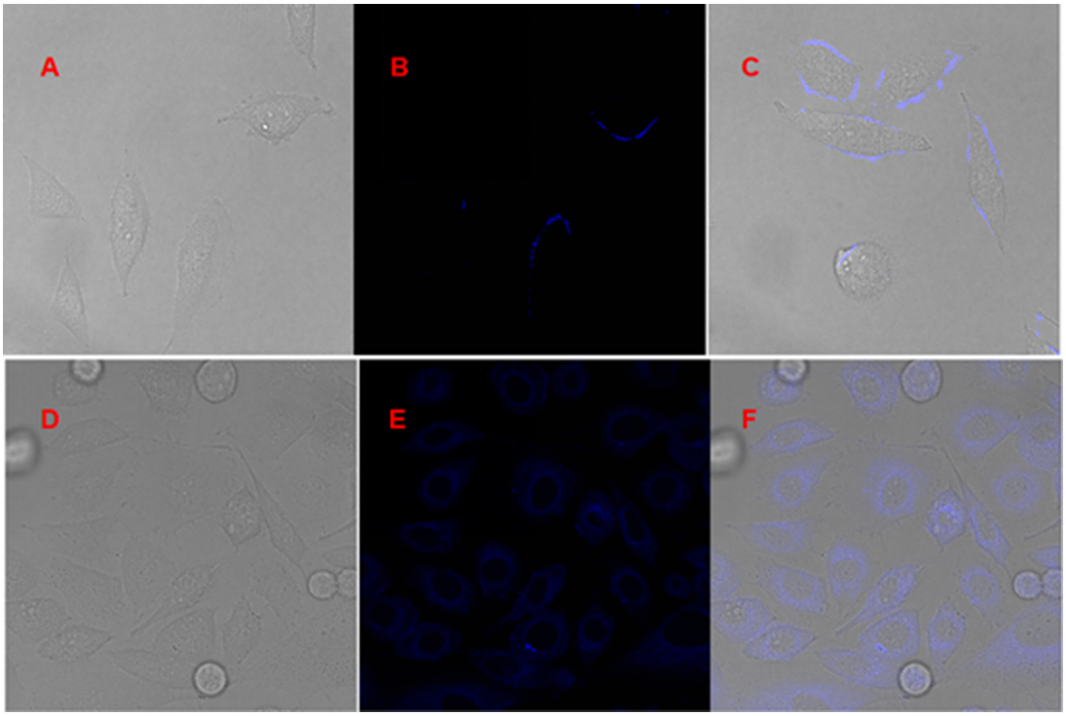

Fig. 7. Fluorescence microscopic images of HepG2 cells: (a) Untreated Cell control; (b) Cells treated with HL; (c) overlap image of (a) and (b); (d) Untreated Cell control; (e) Cells treated with **CETC** and ClO^-; (f) overlap image of (d) and (e).

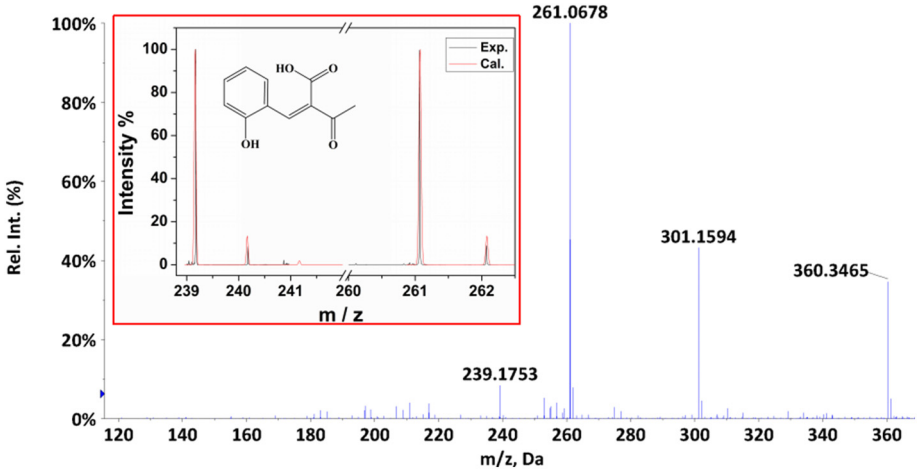

Fig. 8. ESI mass spectra of **ACO** upon addition of excess ClO^-.

(201610324021Z), the Six Talent Peaks Project in Jiangsu Province (SWYY-063) and sponsored by Qing Lan Project of Jiangsu Province.

Appendix A. Supplementary data

Supplementary data to this article can be found online at https://doi.org/10.1016/j.saa.2018.12.019.

References

[1] B.D. Autreaux, M.B. Toledano, ROS as signalling molecules: mechanisms that generate specificity in ROS homeostasis, Nat. Rev. Mol. Cell Biol. 8 (2007) 813–824.
[2] C.C. Winterbourn, Reconciling the chemistry and biology of reactive oxygen species, Nat. Chem. Biol. 4 (2008) 278–286.
[3] J.E. Harrison, J. Schultz, Studies on the chlorinating activity of myeloperoxidase, J. Biol. Chem. 251 (1976) 1371–1374.
[4] X. Chen, K. Lee, X. Ren, J. Ryu, G. Kim, J. Ryu, W. Lee, J. Yoon, Synthesis of a highly HOCl-selective fluorescent probe and its use for imaging HOCl in cells and organisms, J. Nat. Protoc. 11 (2016) 1219–1228.
[5] S.K. Yoo, T.W. Starnes, Q. Deng, A. Huttenlocher, Lyn is a redox sensor that mediates leukocyte wound attraction in vivo, Nature 480 (2011) 109–112.
[6] K.M. Zhang, W. Dou, P.X. Li, R. Shen, J.X. Ru, W. Liu, Y.M. Cui, C.Y. Chen, W.S. Liu, D.C. Bai, A coumarin-based two-photon probe for hydrogen peroxide, Biosens. Bioelectron. 64 (2015) 542–546.
[7] X. Han, C. Tian, J. Jiang, M.S. Yuan, S.W. Chen, J. Xu, T. Li, J. Wang, Two ratiometric fluorescent probes for hypochlorous acid detection and imaging in living cells, Talanta 186 (2018) 65–72.
[8] J.M. Zgliczynski, T. Stelmaszynska, W.O. Ostrowski, J. Naskalski, J. Sznajd, Events related to the phagocytosis of Cryptococcus neoformans by alveolar macrophages, Eur. J. Biochem. 4 (1968) 540–547.
[9] J. Shepherd, S.A. Hilderbrand, P. Waternan, J.W. Heinecke, R. Weissleder, P. Libby, A fluorescent probe for the detection of myeloperoxidase activity in atherosclerosis-associated macrophages, Chem. Biol. 14 (2007) 1221–1231.
[10] J. Zhou, L.H. Li, W. Shi, X.H. Gao, X.H. Li, H.M. Ma, HOCl can appear in the mitochondria of macrophages during bacterial infection as revealed by a sensitive mitochondrial-targeting fluorescent probe, Chem. Sci. 6 (2015) 4884–4888.

[11] W. Shu, L. Yan, Z. Wang, J. Liu, S. Zhang, C. Liu, B. Zhu, A novel visual and far-red fluorescent dual-channel probe for the rapid and sensitive detection of hypochlorite in aqueous solution and living cells, Sensors Actuators B Chem. 221 (2015) 1130–1136.
[12] L. Yuan, W. Lin, J. Song, Y. Yang, Development of an ICT-based ratiometric fluorescent hypochlorite probe suitable for living cell imaging, Chem. Commun. 47 (2011) 12691–12693.
[13] B. Zhu, L. Wu, M. Zhang, Y. Wang, C. Liu, Z. Wang, Q. Duan, P. Jia, A highly specific and ultrasensitive near-infrared fluorescent probe for imaging basal hypochlorite in the mitochondria of living cells, Biosens. Bioelectron. 107 (2018) 218–223.
[14] L.C. Adam, G. Gordon, Direct and sequential potentiometric determination of hypochlorite, chlorite, and chlorate ions when hypochlorite ion is present in large excess, Anal. Chem. 67 (1995) 535–540.
[15] S. Fu, M.J. Davies, R. Stocker, R.T. Dean, Evidence for roles of radicals in protein oxidation in advanced human atherosclerotic plaque, Biochem. J. 333 (1998) 519–525.
[16] A.K. Yadav, A. Bracher, S.F. Doran, M. Leustik, G.L. Squadrito, E.M. Postlethwait, S. Matalon, Mechanisms and modification of chlorine-induced lung injury in animals, Proc. Am. Thorac. Soc. 7 (2010) 278–283.
[17] S.A. Weitzman, L.I. Gordon, Inflammation and cancer: role of phagocyte-generated oxidants in carcinogenesis, Blood 76 (1990) 655–663.
[18] Y.W. Yap, M. Whiteman, N.S. Cheung, Chlorinative stress: an under appreciated mediator of neurodegeneration, Cell. Signal. 19 (2007) 219–228.
[19] Y. Ning, J. Cui, Y. Lu, X. Wang, C. Xiao, S. Wu, J. Li, Y. Zhang, De novo design and synthesis of a novel colorimetric fluorescent probe based on naphthalenone scaffold for selective detection of hypochlorite and its application in living cells, Sensors Actuators B Chem. 269 (2018) 322–330.
[20] A. Daugherty, J.L. Dunn, D.L. Rateri, J.L. Heinecke, Myeloperoxidase, a catalyst for lipoprotein oxidation, is expressed in human atherosclerotic lesions, J. Clin. Invest. 94 (1994) 437–444.
[21] R. Cairns, I. Harris, T. Mak, Regulation of cancer cell metabolism, Nat. Rev. Cancer 11 (2011) 85–95.
[22] J.J. Hu, N. Wong, M. Lu, X. Chen, S. Ye, A.Q. Zhao, P. Gao, R.Y. Kao, J. Shen, D. Yang, HKOCl-3: a fluorescent hypochlorous acid probe for live-cell and in vivo imaging and quantitative application in flow cytometry and a 96-well microplate assay, Chem. Sci. 7 (2016) 2094–2099.
[23] S.M. Wu, S.V. Pizzo, alpha(2)-Macraglobulin from rheumatoid arthritis synovial fluid: functional analysis defines a role for oxidation in inflammation, Arch. Biochem. Biophys. 391 (2001) 119–126.
[24] H. Zhu, J. Fan, J. Wang, H. Mu, X. Peng, An enhanced PET-based fluorescent probe with ultrasensitivity for imaging basal and elesclomol-induced HClO in cancer cells, J. Am. Chem. Soc. 136 (2014) 12820–12823.
[25] Q. Xu, C.H. Heo, J.A. Kim, H.S. Lee, Y. Hu, D. Kim, K.M.K. Swamy, G. Kim, S.J. Nam, H.M. Kim, J. Yoon, A selective imidazoline-2-thione-bearing two-photon fluorescent probe for hypochlorous acid in mitochondria, Anal. Chem. 88 (2016) 6615–6620.
[26] L. Yuan, L. Wang, B.K. Agrawalla, S.J. Park, H. Zhu, B. Sivaraman, J. Peng, Q.H. Xu, Y.T. Chang, Development of targetable two-photon fluorescent probes to image hypochlorous acid in mitochondria and lysosome in live cell and inflamed mouse model, J. Am. Chem. Soc. 137 (2015) 5930–5938.
[27] S. Ding, Q. Zhang, S. Xue, G. Feng, Real-time detection of hypochlorite in tap water and biological samples by a colorimetric, ratiometric and near-infrared fluorescent turn-on probe, Analyst 140 (2015) 4687–4693.
[28] J. Kang, F.J. Huo, Y.K. Yue, Y. Wen, J.B. Chao, Y.B. Zhang, C.X. Yin, A solvent depend on ratiometric fluorescent probe for hypochlorous acid and its application in living cells, Dyes Pigments 136 (2017) 852–858.
[29] D. Li, Y. Feng, J. Lin, M. Chen, S. Wang, X. Wang, H. Sheng, Z. Shao, M. Zhu, X. Meng, A mitochondria-targeted two-photon fluorescent probe for highly selective and rapid detection of hypochlorite and its bio-imaging in living cells, Sensors Actuators B Chem. 222 (2016) 483–491.
[30] X. Chen, F. Wang, J.Y. Hyun, T. Wei, J. Qiang, X. Ren, I. Shin, J. Yoon, Recent progress in the development of fluorescent, luminescent and colorimetric probes for detection of reactive oxygen and nitrogen species, Chem. Soc. Rev. 45 (2016) 2976–3016.
[31] C. Chang, F. Wang, J. Qiang, Z. Zhang, Y. Chen, W. Zhang, Y. Wang, X. Chen, Benzothiazole-based fluorescent sensor for hypochlorite detection and its application for biological imaging, Sensors Actuators B Chem. 243 (2017) 22–28.
[32] Q. Xu, C.H. Heo, G. Kim, H.W. Lee, H.M. Kim, J. Yoon, Development of imidazoline-2-thiones based two-photon fluorescence probes for imaging hypochlorite generation in a co-culture system, Angew. Chem. Int. Ed. 54 (2015) 4890–4894.
[33] S.V. Mulay, M. Choi, Y.J. Jang, Y. Kim, S. Jon, D.G. Churchill, Enhanced fluorescence turn-on imaging of hypochlorous acid in living immune and cancer cells, Chem. Eur. J. 22 (2016) 9642–9648.
[34] L.L. Shi, X. Li, M. Zhou, F. Muhammad, Y.B. Ding, H. Wei, An arylboronate locked fluorescent probe for hypochlorite, Analyst 142 (2017) 2104–2108.
[35] B. Zhu, L. Wu, H. Zhu, Z. Wang, Q. Duan, Z. Fang, P. Jia, Z. Li, C. Liu, A highly specific and ultrasensitive two-photon fluorescent probe for imaging native hypochlorous acid in living cells, Sens. Actuators, B 269 (2018) 1–7.
[36] Z. Zhan, R. Liu, L. Chai, Q. Li, K. Zhang, Y. Lv, Turn-on fluorescent probe for exogenous and endogenous imaging of hypochlorous acid in living cells and quantitative application in flow cytometry, Anal. Chem. 89 (17) (2017) 9544–9551.
[37] X. Jiao, C. Liu, Q. Wang, K. Huang, S. He, L. Zhao, X. Zeng, Fluorescence probe for hypochlorous acid in water and its applications for highly lysosome-targetable live cell imaging, Anal. Chim. Acta 969 (2017) 49–56.
[38] X. Zhang, F. Gao, Imaging mitochondrial reactive oxygen species with fluorescent probes: current applications and challenges, Free Radic. Res. 49 (2015) 374–382.
[39] D.S. Ranade, A.M. Bapat, S.N. Ramteke, B.N. Joshi, P. Roussel, A. Tomas, P. Deschamps, P.P. Kulkarni, Thiosemicarbazone modification of 3-acetyl coumarin inhibits Aβ peptide aggregation and protect against Aβ-induced cytotoxicity, Eur. J. Med. Chem. 121 (2016) 803–809.
[40] J. Chen, W. Liu, J. Ma, H. Xu, J. Wu, X. Tang, Z. Fan, P. Wang, Synthesis and properties of fluorescence dyes: tetracyclic pyrazolo[3,4-b]pyridine-based coumarin chromophores with intramolecular charge transfer character, J. Org. Chem. 77 (7) (2012) 3475–3482.
[41] G. He, J. Li, Z. Wang, C. Liu, X. Liu, L. Ji, C. Xie, Q. Wang, Design and synthesis of a fluorescent probe based on naphthalene anhydride and its detection of copper ions, Tetrahedron 73 (3) (2017) 272–277.
[42] X. Jia, Q. Chen, Y. Yang, Y. Tang, R. Wang, Y. Xu, W. Zhu, X. Qian, FRET-based Mito-specific fluorescent probe for ratiometric detection and imaging of endogenous peroxynitrite: dyad of Cy3 and Cy5, J. Am. Chem. Soc. 138 (2016) 10778–10781.
[43] L. Wang, W. Li, W. Zhi, D. Ye, W. Zhang, L. Ni, Rapid detection of hypochlorite by a coumarin-based hydrazide in aqueous solution and its application in live-cell imaging, Sensors Actuators B Chem. 255 (2018) 1112–1118.
[44] D.S. Ranade, A.M. Bapat, S.N. Ramteke, B.N. Joshi, P. Roussel, A. Tomas, P. Deschamps, P.P. Kulkarni, Thiosemicarbazone modification of 3-acetyl coumarin inhibits Aβ peptide aggregation and protect against Aβ-induced cytotoxicity, Eur. J. Med. Chem. 121 (2016) 803–809.
[45] J. Chen, W. Liu, H. Ma Xu, J. Wu, X. Tang, Z. Fan, P. Wang, Synthesis and properties of fluorescence dyes: tetracyclic pyrazolo[3,4-b]pyridine-based coumarin chromophores with intramolecular charge transfer character, J. Org. Chem. 77 (7) (2012) 3475–3482.
[46] W.L. Wu, X. Zhao, L.L. Xi, M.F. Huang, W.H. Zeng, J.Y. Miao, B.X. Zhao, A mitochondria-targeted fluorescence probe for ratiometric detection of endogenous hypochlorite in the living cells, Anal. Chim. Acta 950 (2017) 178–183.
[47] J. Li, X. Yang, D. Zhang, Y. Liu, J. Tang, Y. Li, Y. Zhao, Y. Ye, A fluorescein-based "turn-on" fluorescence probe for hypochlorous acid detection and its application in cell imaging, Sensors Actuators B Chem. 265 (2018) 84–90.
[48] L. Chen, S.J. Park, D. Wu, H.M. Kim, J. Yoon, A two-photon ESIPT based fluorescence probe for specific detection of hypochlorite, Dyes Pigments 158 (2018) 526–532.